ISSN 1674-1056
http://cpb.iphy.ac.cn
http://iopscience.iop.org/cpb
中国物理 B
Chinese Physics
中国物理
Chinese Physics B

Vibrational modes in $La_2Zr_2O_7$ pyrochlore irradiated with disparate electrical energy losses

Sheng-Xia Zhang(张胜霞), Jie Liu(刘杰), Hua Xie(谢华), Li-Jun Xu(徐丽君), Pei-Pei Hu(胡培培), Jian Zeng(曾健), Zong-Zhen Li(李宗臻), Li Liu(刘丽), Wen-Si Ai(艾文思), Peng-Fei Zhai(翟鹏飞)
Citation: Chin. Phys. B . 2019, 28(11): 116102 . **doi:** 10.1088/1674-1056/ab43bf
Journal homepage: http://cpb.iphy.ac.cn; http://iopscience.iop.org/cpb

What follows is a list of articles you may be interested in

Effects of temperature and point defects on the stability of C15 Laves phase in iron: A molecular dynamics investigation

Hao Wang(王昊), Ning Gao(高宁), Guang-Hong Lü(吕广宏), Zhong-Wen Yao(姚仲文)
Chin. Phys. B . 2018, 27(6): 066104 . **doi:** 10.1088/1674-1056/27/6/066104

Compression behavior and phase transition of β-Si_3N_4 under high pressure

Hong-xia Gong(龚红霞), Zi-li Kou(寇自力), Cong Fan(樊聪), Hao Liang(梁浩), Qi-ming Wang(王齐明), Lei-lei Zhang(张雷雷), Fang Peng(彭放), Ming Yang(杨鸣), Xiao-lin Ni(倪小林), Jing Liu(刘景)
Chin. Phys. B . 2018, 27(5): 056101 . **doi:** 10.1088/1674-1056/27/5/056101

Structural modification in swift heavy ion irradiated muscovite mica

Sheng-Xia Zhang(张胜霞), Jie Liu(刘杰), Jian Zeng(曾健), Pei-Pei Hu(胡培培), Peng-Fei Zhai(翟鹏飞)
Chin. Phys. B . 2017, 26(10): 106102 . **doi:** 10.1088/1674-1056/26/10/106102

Comparison of total dose effects on SiGe heterojunction bipolar transistors induced by different swift heavy ion irradiation

Sun Ya-Bin, Fu Jun, Xu Jun, Wang Yu-Dong, Zhou Wei, Zhang Wei, Cui Jie, Li Gao-Qing, Liu Zhi-Hong
Chin. Phys. B . 2014, 23(11): 116104 . **doi:** 10.1088/1674-1056/23/11/116104

Single event effect in a ferroelectric-gate field-effect transistor under heavy-ion irradiation

Yan Shao-An, Tang Ming-Hua, Zhao Wen, Guo Hong-Xia, Zhang Wan-Li, Xu Xin-Yu, Wang Xu-Dong, Ding Hao, Chen Jian-Wei, Li Zheng, Zhou Yi-Chun
Chin. Phys. B . 2014, 23(4): 046104 . **doi:** 10.1088/1674-1056/23/4/046104

Vibrational modes in $La_2Zr_2O_7$ pyrochlore irradiated with disparate electrical energy losses*

Sheng-Xia Zhang(张胜霞)[1,†], Jie Liu(刘杰)[1,‡], Hua Xie(谢华)[2], Li-Jun Xu(徐丽君)[1,3], Pei-Pei Hu(胡培培)[3], Jian Zeng(曾健)[1], Zong-Zhen Li(李宗臻)[1,3], Li Liu(刘丽)[1,3], Wen-Si Ai(艾文思)[1,3], and Peng-Fei Zhai(翟鹏飞)[1]

[1] *Institute of Modern Physics, Chinese Academy of Sciences (CAS), Lanzhou* 730000, *China*

[2] *Fundamental Science on Nuclear Wastes and Environmental Safety Laboratory, Southwest University of Science and Technology, Mianyang* 621010, *China*

[3] *University of Chinese Academy of Sciences, Beijing* 100049, *China*

(Received 23 July 2019; revised manuscript received 10 September 2019; published online 16 October 2019)

Polycrystalline samples of $La_2Zr_2O_7$ pyrochlore are irradiated by different energetic heavy ions to investigate the dependence of the vibrational mode variations on the irradiation parameters. The applied electronic energy loss $(dE/dx)_e$ increases from about 5.2 keV/nm to 39.6 keV/nm. The ion fluence ranges from 1×10^{11} ions/cm^2 to 6×10^{15} ions/cm^2. Vibrational modes of irradiated pyrochlore are analyzed by using Raman spectrum. Infrared active modes F_{1u} at 192, 308, and 651 cm^{-1} appear in Raman spectra, and the F_{2g} band at 265 cm^{-1} rises up due to the irradiation by 200-MeV Kr ions with $(dE/dx)_e$ of 16.0 keV/nm. Differently, for the pyrochlore irradiated by 1750-MeV Bi ions with $(dE/dx)_e$ of 39.6 keV/nm, in spite of the appearance of infrared active mode F_{1u} 651 cm^{-1}, the amorphous structure occurs according to the vibrational mode variations of pyrochlore irradiated at higher ion fluences. Amorphous tracks are observed in the samples, which confirm the occurrence of pyrochlore–amorphous transition in pyrochlore irradiated with $(dE/dx)_e$ of 39.6 keV/nm.

Keywords: pyrochlore, heavy ion irradiation, vibrational spectra, phase transition

PACS: 61.80.–x, 61.82.–d **DOI:** 10.1088/1674-1056/ab43bf

1. Introduction

Pyrochlore, as a fast-ion conductor for electrolytes in solid oxide fuel cells,[1] frustrated magnetism,[2] ferroelectricity,[3] photocatalys,[4] photoluminescence,[5] has aroused the great interest of all. Besides, $A_2B_2O_7$ pyrochlore has great attraction in present nuclear technology as a material for disposal of nuclear wastes, due to its ability to accommodate minor actinides and an excellent resistance to radiation in the nuclear stopping regime. Pyrochlore has a superstructure of the fluorite structure-type with the A-site and B-site cations ordered and one-eighth of the anions missing.[6,7] Two different oxygen sites occur in pyrochlore: the 48f sites (0.75-x, 1/8, 1/8) that are occupied by six oxygen atoms (O), and the 8a site (1/8, 1/8, 1/8) where the seventh oxygen atom (O′) is located.[6–8] Fantastic properties of pyrochlore originate particularly from the presence of one vacant site per eight oxygen sites that could provide fast channels for oxygen diffusion.[8]

The response of pyrochlore to the extreme conditions has received a great deal of attention. Heavy ion irradiation is usually used to simulate harsh irradiation environment of materials.[9–11] Heavy ion irradiation has been applied to pyrochlore for precision micromachining, forming nanostructures, processing thin films, and inducing phase transitions. Interestingly, it is found that the phase transition and the microstructure during heavy ion irradiation are varied with the chemical composition of pyrochlore.[12–16] Quite a lot of researches have been conducted on the binary $Gd_2Zr_{2-x}Ti_xO_7$ pyrochlore.[17–20] It is indicated that the resistance to irradiation-induced amorphization significantly increases with the Zr-content. Rare earth titanate $Gd_2Ti_2O_7$ undergoes a pyrochlore-to-amorphous transition. Whereas $Gd_2Zr_2O_7$ is transformed into an anion-defect fluorite structure. Actually, the cationic radius ratio r_A/r_B of pyrochlore governs the stability of the pyrochlore structure.[16,21–23] It is reported that in the ambient conditions, the pyrochlore is stable as its r_A/r_B ranges from 1.46 to 1.78. A disordered fluorite structure can be formed as the r_A/r_B drops below 1.46. While the structure will exhibit a monoclinic, layered-perovskite structure when its r_A/r_B is above 1.78.[21] The cation ionic ratio r_A/r_B of $La_2Zr_2O_7$ pyrochlore is about 1.61. Chartier *et al.* have shown that $La_2Zr_2O_7$ has a greater tendency toward cation disorder.[24] It is thought that $La_2Zr_2O_7$ should be "resistant" to radiation damage by simply disordering to the defect fluorite structure rather than becoming amorphous structure.[14,24] Moreover, physical properties of the materials are strongly dependent on the structural stability. Sattonnay *et al.* found that the evolution of the mechanical properties of swift heavy ion irradiated pyrochlore depends on the residual

*Project supported by the National Natural Science Foundation of China (Grant Nos. 11705246, 11675233, and 11690041) and the Natural Science Foundation of Gansu Province, China (Grant No. 17JR5RA316).

†Corresponding author. E-mail: zhangsx@impcas.ac.cn

‡Corresponding author. E-mail: j.liu@impcas.ac.cn

© 2019 Chinese Physical Society and IOP Publishing Ltd

stress introduced into the sample surface layer.[25,26] Sellami *et al.* observed that the thermal conductivity decreases in irradiated $Gd_2Ti_2O_7$ and $Y_2Ti_2O_7$.[27] In this work, $La_2Zr_2O_7$ pyrochlore is exposed to energetic heavy ion irradiation with different ion fluences and $(dE/dx)_e$ varying from 5.2 keV/nm to 39.6 keV/nm. The vibrational modes of irradiated $La_2Zr_2O_7$ pyrochlore are investigated to find out the dependence of structural transition on irradiation parameters.

2. Experiment

2.1. $La_2Zr_2O_7$ pyrochlore preparation

$La_2Zr_2O_7$ pyrochlore pellets were prepared by a sol–gel method with an aqueous mixture of zirconium nitrate solutions $Zr(NO_3)_4{\cdot}3H_2O$ and appropriate rare-earth nitrate $La(NO_3)_3{\cdot}6H_2O$. Citric acid was used as the complexing agent. Each standard solution was accurately measured and mixed according to Table 1. The mixed solution was stirred for 0.5 h–2 h at room temperature. In the stirring process, the pH of the mixture was adjusted to 5 by using ammonia water. The obtained transparent sol was atomized into corundum crucible as sample precursor. The precursor was first kept at 1173 K to remove the volatile substances. After that, the precursor was calcined for 12 h at 1673 K and kept at 1400 K for 36 h to obtain the bulk $La_2Zr_2O_7$ pyrochlore.

Table 1. Detailed chemical design for $La_2Zr_2O_7$ pyrochlore.

Formula	Volume of solution/ml		Additive/g	
	$La(NO_3)_3$	$Zr(NO_3)_4$	Polyethylene glycol	Citric acid
$La_2Zr_2O_7$	400	400	40	64

2.2. Irradiation conditions

$La_2Zr_2O_7$ samples were irradiated at room temperature with various kinds of heavy ions (*e.g.*, Ar, Kr, Bi) accelerated by the heavy ion research facility in Lanzhou (HIRFL) at fluences ranging from 1×10^{11} ions/cm^2 up to 6×10^{15} ions/cm^2. The ion flux was always kept lower than 5 ions/(cm^2·s)–8×10^8 ions/(cm^2·s) to avoid overheating. The electronic energy loss $(dE/dx)_e$ near the surface of the irradiated $La_2Zr_2O_7$ increased from about 5.2 keV/nm to 39.6 keV/nm. All irradiated experiments were performed in vacuum at room temperature. The detailed parameters, *e.g.*, $(dE/dx)_e$, were calculated by SRIM 2010 code,[28] as shown in Table 2.

Table 2. Detailed parameters applied in this experiment.

Ion	Energy/MeV	$(dE/dx)_e$/(keV/nm)	$(dE/dx)_n$/(keV/nm)	Ion fluences/(ions/cm^2)	Projected range/μm
Ar	260	5.2	3.5×10^{-3}	6×10^{14}–6×10^{15}	42.1
Kr	1980	9.1	4.5×10^{-3}	1×10^{11}–5×10^{12}	150.5
Kr	200	16.0	3.1×10^{-2}	6×10^{14}–6×10^{15}	16.7
Bi	1750	39.6	5.1×10^{-2}	5×10^{11}–3×10^{12}	52.3

2.3. Measurements

A Microscopic confocal Raman spectrometer (Lab RAM HR800, Jobin Yvon Co.) was used to analyze the vibrational modes of irradiated $La_2Zr_2O_7$ pyrochlore at room temperature. The laser excitation wavelength was 532 nm. Raman shift from 150 cm^{-1} to 1000 cm^{-1} was chosen for this experiment. The total exposure time was 30 s for each sample.

Focus ion beam system (FIB, Helios Nanolab 600, FEI) was used to prepare the samples for cross-sectional observation of microstructure. The depth of the prepared sample was about 5.5 μm from the irradiated surface. The specimen prepared by FIB was examined by using transmission electron microscope (TEM, 2100 F, JEOL) to observe the profiles of the nano structure of the irradiated samples. The TEM was operated at 200 kV.

3. Results and discussion

Raman spectroscopy is highly sensitive to metal-oxygen vibrational modes. In Raman spectrum, La and Zr atoms in $La_2Zr_2O_7$ pyrochlore do not contribute to the Raman active vibrations because they are located at the inversion center.[6,29] Raman activity of pyrochlore results from oxygen vibrations. The Raman spectrum of $La_2Zr_2O_7$ pyrochlore is similar to that of other $A_2B_2O_7$ pyrochlore with six Raman active vibrational modes. They are $A_{1g}+E_g+4F_{2g}$. Five obvious bands are observed in the Raman spectra of pristine $La_2Zr_2O_7$ as shown in Fig. 1. They are the A_{1g} mode at $\sim$ 493 cm^{-1}, the E_g mode at $\sim$ 300 cm^{-1}, and three F_{2g} bands at $\sim$ 394 cm^{-1}, 515 cm^{-1}, and a weak peak at about 596 cm^{-1}. The assignment of different modes was reported elsewhere.[30–33] The most prominent E_g mode is contributed by O–Zr–O bending vibration with $\sim$ 34% of the potential energy distribution (PED), while $\sim$ 24% of PED is due to La–O stretching vibration.[6,29,33,34] This band is complex containing a strong E_g mode and a weak F_{2g} mode, which are mainly due to the vibration of oxygen in ZrO_6 octahedron. The A_{1g} mode is associated with the O–Zr–O bending vibrations of ZrO_6 octahedron.[6,29,33] Three F_{2g} modes at $\sim$ 394, 515 and 596 cm^{-1} are mostly contributed by the distortions of ZrO_6 octahedron.[6,29,33]

In this work, heavy ions with different energy are used to irradiate $La_2Zr_2O_7$ pyrochlore to investigate the influences of irradiation parameters on vibrational modes' variations of

$La_2Zr_2O_7$. It is observed that no substantial changes appear on the main vibrational modes when $La_2Zr_2O_7$ is irradiated by 260 MeV Ar and 1980-MeV Kr ions with $(dE/dx)_e$ of 5.2 keV/nm and 9.1 keV/nm, respectively, and the results are shown in Fig. 1.

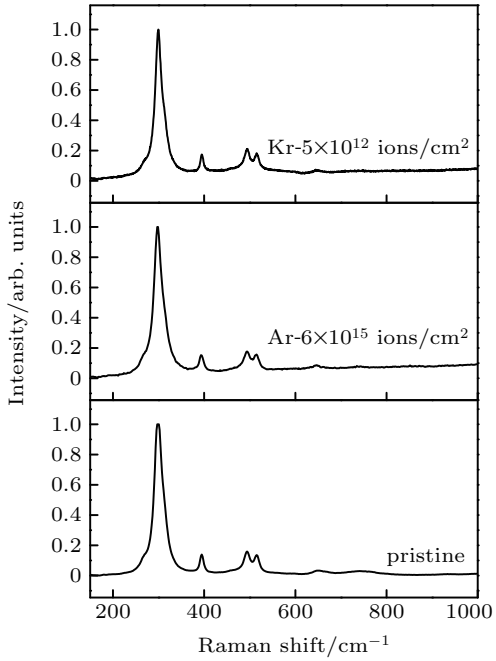


Fig. 1. Raman spectra of $La_2Zr_2O_7$ pyrochlore samples irradiated by 260-MeV Ar and 1980-MeV Kr ions.

Figure 2 exhibits the normalized Raman spectra of $La_2Zr_2O_7$ pyrochlore irradiated by 200-MeV Kr ions with $(dE/dx)_e$ of 16.0 keV/nm at fluences ranging from 6×10^{14} ions/cm^2 to 6×10^{15} ions/cm^2. Lorenz-shaped peaks are fitted to the Raman spectrum. Full width at half maximum (FWHM) and normalized intensity of the fitted bands are depicted in Figs. 2(b) and 2(c). It is interesting that new peaks are generated in the Raman spectrum of $La_2Zr_2O_7$ irradiated with Kr ions. Modes at wavenumbers 192 cm^{-1} and 265 cm^{-1} rise up in the Raman spectra of $La_2Zr_2O_7$ pyrochlore irradiated by Kr ions. Besides, it is found that the mode at about 308 cm^{-1} rises up in the fitted spectrum of irradiated pyrochlore. The band at wavenumber 265 cm^{-1} is assigned to the remaining F_{2g} mode due to O–Zr–O vibration mixed with La–O′ bending vibration. It is not possible to unambiguously assign the low wavenumber Raman mode at 192 cm^{-1} in Kr ion irradiated pyrochlore. Possibilities may include one of the defect-activated Raman forbidden F_{1u} modes. Infrared mode F_{1u} at 192 cm^{-1} is caused by the vibrations of Zr–LaO_6 due to Zr–O and La–O stretching vibration mixed with O–La–O bending vibration.[34] The mode at 308 cm^{-1} could be assigned to the infrared mode F_{1u}, which is caused by La–O′ and O-O′ vibration.[34] The selection rules result in some vibrational modes being optically inactive based on symmetry.[35] Random displacement disorder can result in the relaxation of the selection rules, and previously inactive Raman modes are expected to appear in Raman spectra.[35,36] Hence, it is assumed that 200-MeV Kr ion irradiation induces the La and O′ sites to be displaced in pyrochlore.

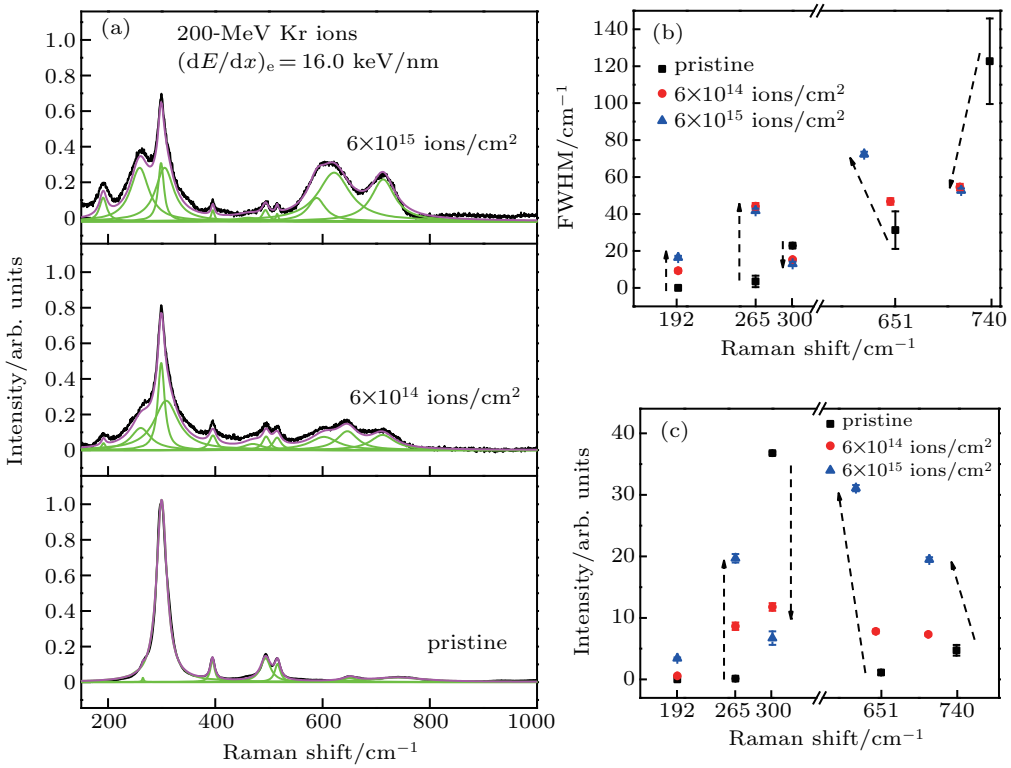


Fig. 2. (a) Plots of intensity *versus* Raman shift of $La_2Zr_2O_7$ pyrochlore samples irradiated by 200-MeV Kr ions with $(dE/dx)_e$ of 16.0 keV/nm at various fluences. Dependence of (b) FWHM and (c) relative intensity of band on Raman shift of $La_2Zr_2O_7$ pyrochlore samples irradiated by different ion fluences.

According to Fig. 2, the intensity of the band at 651 cm^{-1} and 740 cm^{-1} increase with ion fluence increasing. The band at wavenumber 651 cm^{-1} is assigned to be infrared active F_{1u} mode related to a mixture of La–O and Zr–O bond stretching with bending vibrations.[6,29–34] It is noted that wavenumber at 740 cm^{-1} is assigned to be of amorphous mode. It is suggested that disordered structure occurs in the pyrochlore irradiated with higher ion fluence.[35] In addition, the frequency of modes at 651 cm^{-1} and 740 cm^{-1} shift towards lower wavenumbers with ion fluence increasing, according to Fig. 2. Raman shift is related to the structure of the target material. It is thought that the octahedron deformation occurs in the pyrochlore due to Kr ion irradiation. Infrared active mode F_{1u} shifting towards lower frequency indicates that the energy needed for photon to vibrate is lower, suggesting that the observed structure becomes unstable due to the irradiation of heavy ions.

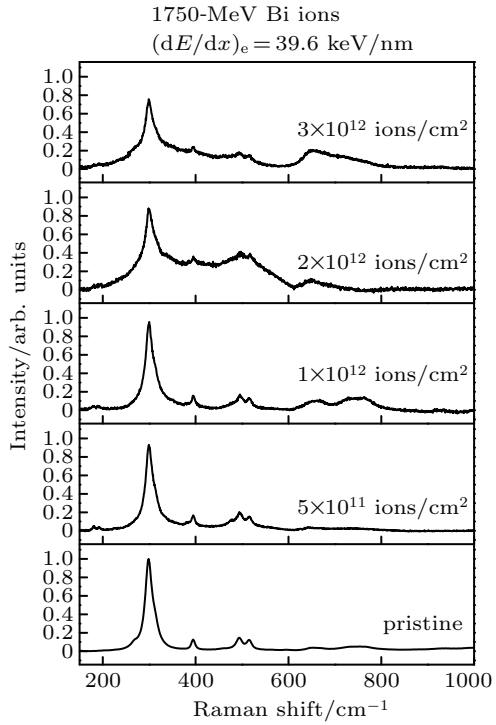


Fig. 3. Plots of intensity *versus* Raman shift of $La_2Zr_2O_7$ pyrochlore recorded before and after the irradiation of Bi ions with 39.6 keV/nm at various fluences.

The influences of irradiation parameters on the vibrational modes of $La_2Zr_2O_7$ pyrochlore are further verified. The $La_2Zr_2O_7$ pyrochlore sample is subjected to the irradiation of 1750-MeV Bi ions ($(dE/dx)_e = 39.6$ keV/nm). Figure 3 shows the normalized Raman spectrum of $La_2Zr_2O_7$ pyrochlore irradiated by Bi ions with increasing fluences. After being irradiated by Bi ions with increasing fluences, all crystalline vibrational modes broaden in width and decrease in intensity. It is indicated that swift heavy ion irradiation introduces an amorphous structure into $La_2Zr_2O_7$ pyrochlore. This behavior has also been observed in other irradiated pyrochlores. No shift occurs towards the strongest peak at 300 cm^{-1} as marked by the dash line in Fig. 3. The F_{1u} mode at 192 cm^{-1} is not present in Bi ion irradiated pyrochlore. A broad peak-like structure with a maximum at $\sim$ 740 cm^{-1} is still existent, which has been observed in 200-MeV Kr ion experiments and is related to the formation of amorphous phase. Another F_{1u} mode at $\sim$ 651 cm^{-1} exists over the entire fluence range, and the peak intenstity increases and the peak width broadens with fluence increasing. At higher ion fluence 3×10^{12} ions/cm^2, the peaks at 651 cm^{-1} and 740 cm^{-1} are combined into a broad peak. It is suggested that amorphous fraction in the irradiated pyrochlore increases with ion fluence increasing. Quantitative analysis of the peaks is not made because the background noise grows up with fluence increasing. Nevertheless, the evolution of the intensity profiles comfirme that the intensities of the crystalline vibrational modes decrease systematically with fluence increasing.

To observe the detailed microstructure of the irradiated pyrochlore, TEM is used to explore the pyrochlore irradiated by Bi ion with $(dE/dx)_e$ of 39.6 keV/nm. As expected, continuous tracks with amorphous structure in the core are found as shown in Fig. 4. Figure 4(b) shows the magnified image of the track at about 5 μm far from the irradiated surface. The structure in the track core is amorphous and surrounded by defect fluorite shell. The TEM morphology of the amorphous tracks also verifies the results shown in Fig. 3. The core–shell morphology shows the general structure of the latent tracks caused by heavy ion irradiation in pyrochlore. Previous literature has reported the latent tracks consisted with fluorite and amorphous structures.[19,37,38] An amorphous core surrounded by an anion-deficient fluorite shell has a well-known core–shell structure of the latent tracks in heavy ion irradiated pyrochlore. The core–shell morphology of the latent tracks is associated with the localized "melting" and rapid recrystallization process following heavy ion penetration.[38] According to the thermal spike model, the rapid quenching of a "molten" zone give rise to the amorphous core, while the epitaxial recrystallization at the molten/solid interface produces a surrounding shell. Multiple factors determine the final morphology of the latent tracks in irradiated pyrochlore. On the one hand, the energy density and the cooling rate strongly influence the track morphology. Rapid cooling leads to an amorphous track core, while the slower cooling will cause the disordered structure to form. High energy density induced by Bi ions with higher $(dE/dx)_e$ leads to a rapid cooling rate along the ion path. Thus, amorphous track core is observed in the Bi ion irradiated $La_2Zr_2O_7$ pyrochlore. On the other hand, the final structure of ion tracks depends on the competition between melting process and recrystallization process, which is dependent on the chemical composition of pyrochlores, in particular, the cation ionic radius r_A/r_B.[39] The amorphous core becomes larger, and the defect shell becomes less pronounced

with r_A/r_B increasing.

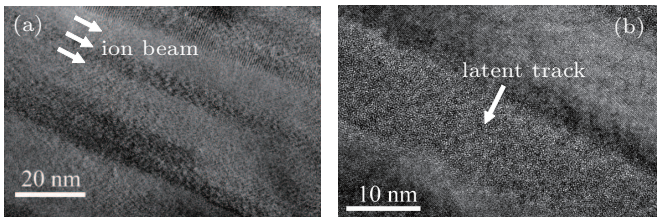


Fig. 4. (a) Cross-section morphology of $La_2Zr_2O_7$ pyrochlore irradiated by Bi ions with $(dE/dx)_e$ of 39.6 keV/nm at fluence of 1×10^{12} ions/cm^2. (b) Morphology of tracks at about 5 μm far from the irradiated surface in high resolution.

4. Conclusions

In this wrok, $La_2Zr_2O_7$ bulk samples are irradiated by various kinds of heavy ions (*e.g.*, Ar, Kr, Bi) in a large energy regime in HIRFL to systematically study the vibrations and phase transitions in heavy ion irradiated pyrochlore. For $La_2Zr_2O_7$ pyrochlore irradiated with $(dE/dx)_e$ of 16.0 keV/nm, infrared modes F_{1u} at wavenumbers 192, 308, and 651 cm^{-1} appear in Raman spectra due to the irradiation induced atom displacement and octahedron deformation. The F_{2g} band at 265 cm^{-1} rises up due to oxygen diffusion or adsorption caused by ion irradiation. For $La_2Zr_2O_7$ pyrochlore irradiated with higher $(dE/dx)_e$, *e.g.*, 39.6 keV/nm, pyrohlore–amorphous transition occurs according to Raman study. The TEM measurements of Bi ion irradiated pyrochlore verify the generation of latent track with amorphous structure in the core.

Acknowledgment

We would like to thank all the accelerator staff of HIRFL of Institute of Modern Physics, Chinese Academy of Sciences (CAS) for their help.

References

[1] Pirzada M, Grimes R W, Minervini L, Maguire J F and Sickafus K E 2001 *Solid State Ionics* **140** 201
[2] Singh D K and Lee Y S 2012 *Phys. Rev. Lett.* **109** 247201
[3] Pasciak M, Wolcyrz M, Pietraszko A and Leoni S 2010 *Phys. Rev. B* **81** 014107
[4] Uno M, Kosuga A, Okui M, Horisaka K and Yamanaka S 2006 *J. Alloys Compd.* **420** 291
[5] Zhang A, Lü M, Zhou G, Wang S and Zhou Y 2006 *J. Phys. Chem. Solids* **67** 2430
[6] Subramanian M A, Aravamudan G and Subba Rao G V 1983 *Prog. Solid St. Chem.* **15** 55
[7] Chakoumakos B C 1984 *J. Solid State Chem.* **53** 120
[8] Aidhy D S, Sachan R, Zarkadoula E, Pakarinen O, Chisholm M F, Zhang Y W and Weber W J 2015 *Sci. Rep.* **5** 16297
[9] Du Y F, Cui L J, Li J S, Li R R and Wan F R 2018 *Acta Phys. Sin.* **67** 216101 (in Chinese)
[10] Hao Z H, Wang H Y, Zhang Q and Mo Z Q 2018 *Acta Phys. Sin.* **67** 247502 (in Chinese)
[11] Wang K, Qi Q, Cheng G J and Shi L Q 2014 *Chin. Phys. Lett.* **31** 072801
[12] Lian J, Wang L M, Wang S X, Chen J, Boatner L A and Ewing R C 2001 *Phys. Rev. Lett.* **87** 145901
[13] Begg B D, Hess N J, McCready D E, Thevuthasan S and Weber W J 2001 *J. Nucl. Mater.* **289** 188
[14] Lian J, Zu X T, Kutty K V G, Chen J, Wang L M and Ewing R C 2002 *Phys. Rev. B* **66** 054108
[15] Lian J, Wang L, Chen J, Sun K, Ewing R C, Farmer J M and Boatner L A 2003 *Acta Mater.* **51** 1493
[16] Sickafus K E, Minervini L, Grimes R W, Valdez J A, Ishimaru M, Li F, McClellan K J and Hartmann T 2000 *Science* **289** 748
[17] Zhang J M, Lang M, Ewing R C, Devanathan R, Weber W J and Toulemonde M 2010 *J. Mater. Res.* **25** 1344
[18] Zhang J W, Lang M, Ewing R C and Becker U 2013 *J. Phys.: Condens. Matter.* **25** 135001
[19] Lang M, Lian J, Zhang J M, Zhang F X, Weber W J, Trautmann C, Neumanna R and Ewing R C 2009 *Phys. Rev. B* **79** 224105
[20] Patel M K, Vijayakumar V, Avasthi D K, Kailas S, Pivin J C, Grover V, Mandal B P and Tyagi A K 2008 *Nucl. Instrum. Methods Phys. Res. Sect. B* **266** 2898
[21] Zhang F X, Lian J, Becker U, Ewing R C, Wang L M, Hu J Z and Saxena S K 2007 *J. Solid State Chem.* **180** 571
[22] Park S, Lang M, Tracy C L, Zhang J M, Zhang F X, Trautmann C, Rodriguez M D, Kluth P and Ewing R C 2015 *Acta Mater.* **93** 1
[23] Sickafus K E, Grimes R W, Valdez J A, Cleave A, Tang M, Ishimaru M, Corish S M, Stanek C R and Uberuaga B P 2007 *Nat. Mater.* **6** 217
[24] Charties A, Meis C, Weber W J and Corrales L R 2002 *Phys. Rev. B* **65** 134116
[25] Sattonnay G, Moll S, Desbrosses V, Menvie Bekale V, Legros C, Thomé L and Monnet I 2010 *Nucl. Instrum. Methods Phys. Res. Sect. B* **268** 3040
[26] Sattonnay G, Moll S, Herbst-Ghysel M, Legros C, Costantini J M and Thomé L 2008 *Nucl. Instrum. Methods Phys. Res. Sect. B* **266** 3052
[27] Sellami N, Sattonnay G, Grygiel C, Monnet I, Debelle A, Legros C, Menut D, Miro S, Simon P, Bechade J L and Thomé L 2015 *Nucl. Instrum. Methods Phys. Res. Sect. B* **365** 371
[28] Ziegler J F, Ziegler M D and Biersack J P 2010 *Nucl. Instrum. Methods Phys. Res. Sect. B* **268** 11
[29] Kong L, Karatchevtseva I, Gregg D J, Blackford M G, Holmes R and Triani G 2013 *J. Am. Ceram. Soc.* **96** 935
[30] Michel D, Jorba M P Y and Collongues R 1976 *J. Raman Spectrosc.* **5** 163
[31] Scheetz B E and White W B 1979 *J. Am. Ceram. Soc.* **62** 468
[32] Vandenborre M T and Husson E 1983 *J. Solid State Chem.* **50** 362
[33] Mandal B P, Krishna P S R and Tyagi A K 2010 *J. Solid State Chem.* **183** 41
[34] Nandi S, Jana Y M and Gupta H C 2018 *J. Phys. Chem. Solids* **115** 347
[35] Long D A 1977 *Raman Spectroscopy* (New York: McGraw-Hill International Book) p. 65
[36] Arenas D J, Gasparov L V, Qiu W, Nino J C, Patterson Charles H and Tanner D B 2010 *Phys. Rev. B* **82** 214302
[37] Zhang J, Lang M, Lian J, Liu J, Trautmann C, Della-Negra S, Toulemonde M and Ewing R C 2009 *J. Appl. Phys.* **105** 113510
[38] Shambin J, Tracy C L, Ewing R C, Zhang F X, Li W X, Trautmann C and Lang M 2016 *Acta Mater.* **117** 207
[39] Sattonnay G, Grygiel C, Monnet I, Legros C, Herbst-Ghysel M and Thomé L 2012 *Acta Mater.* **60** 22